Journal of Controlled Release 291 (2018) 157–168

Contents lists available at ScienceDirect

Journal of Controlled Release

journal homepage: www.elsevier.com/locate/jconrel

Protamine nanocapsules as carriers for oral peptide delivery

Lungile Nomcebo Thwala[a,b], Diego Pan Delgado[a], Kevin Leone[c], Ilaria Marigo[c], Federico Benetti[d], Miguel Chenlo[e], Clara V. Alvarez[e], Sulay Tovar[f], Carlos Dieguez[f], Noemi Stefania Csaba[a,*], Maria Jose Alonso[a,*]

[a] NanobioFar Group, Centre for Research in Molecular Medicine and Chronic Diseases (CIMUS), Universidad de Santiago de Compostela, 15706 Santiago de Compostela, Spain
[b] Université Catholique de Louvain, Louvain Drug Research Institute, Advanced Drug Delivery and Biomaterials, 1200 Brussels, Belgium
[c] Veneto Institute of Oncology IOV-IRCCS, Padua, Italy
[d] ECSIN-European Centre for the Sustainable Impact of Nanotechnology, ECAMRICERT srl, VialePorta Adige, 45, I-45100 Rovigo, Italy
[e] Neoplasia and Endocrine Differentiation Group, Centre for Research in Molecular Medicine and Chronic Diseases (CIMUS), Universidad de Santiago de Compostela, 15706 Santiago de Compostela, Spain
[f] Biomedical Research Group, Centre for Research in Molecular Medicine and Chronic Diseases (CIMUS), Universidad de Santiago de Compostela, 15706 Santiago de Compostela, Spain

ARTICLE INFO

Keywords:
Protamine
Nanocapsules
Oral peptide delivery
Oral peptide absorption
Peptide stability

ABSTRACT

Peptides represent a promising therapeutic class with the potential to alleviate many severe diseases. A key limitation of these active molecules relies on the difficulties for their efficient oral administration. The objective of this work has been the rational design of polymer nanocapsules (NCs) intended for the oral delivery of peptide drugs. For this purpose, we selected insulin glulisine as a model peptide. The polymer shell of the NCs was made of a single layer of protamine, a cationic polypeptide selected for its cell penetration properties, or a double protamine/polysialic acid (PSA) layer. Insulin glulisine-loaded protamine and protamine/PSA NCs, prepared by the solvent displacement method, exhibited a size that varied in the range of 200–400 nm and a neutral surface charge (from +8 mV to −6 mV), depending on the formulation. The stability of the encapsulated peptide was assessed using circular dichroism and an *in vitro* cell activity study. Colloidal stability studies were also performed in simulated intestinal media containing enzymes and the results indicated that protamine NCs were stable and able to protect insulin from the harsh intestinal environment, and that this capacity could be further enhanced with a double PSA-Protamine layer. These NCs were freeze-dried and stored at room temperature without alteration of the physicochemical properties. When the insulin-loaded protamine NCs were administered intra-intestinally to diabetic rats (12 h fasting) it resulted in a prolonged glucose reduction (60%) as compared to the control insulin solution. This work raises prospects that protamine NCs may have a potential as oral peptide delivery nanocarriers.

1. Introduction

The number of peptide drugs in the industry pipelines has significantly increased in the last decades due to their high therapeutic efficacy. Unfortunately, their exploitation has been counter-limited by their difficulties for crossing barriers and, hence, by their necessity of being administered by parenteral routes [1]. Advances in nanomedicine have opened new opportunities for the oral delivery of biomolecules [2] with tremendous efforts dedicated to improving permeation of proteins/peptides through the epithelial membranes whilst protecting them against enzymatic degradation [3]. Indeed, a variety of nanocarriers, among them, liposomes [4], nanogels [5], polymeric nanoparticles (NPs) [6–8] and nanocapsules (NCs) [9], have been reported to protect peptides from the adverse conditions in the (gastrointestinal) GI tract and enhance their transport across the intestinal mucosa. Having as a reference the original work by Damgé et al. [10], which showed for the first time the possibility to enhance insulin absorption using poly(cyanoacrylate) NCs, our group explored the potential of chitosan NCs for the oral administration of salmon calcitonin [11]. The positive results were attributed not only to the composition of these NCs but also to their structural organization. NCs are composed of a core, which may act as a protective reservoir for the drug, and a surrounding shell [12], which can be rationally designed in order to confer the NCs with adequate stability, mucodiffusion, and

* Corresponding authors.
E-mail addresses: noemi.csaba@usc.es (N.S. Csaba), mariaj.alonso@usc.es (M.J. Alonso).

https://doi.org/10.1016/j.jconrel.2018.10.022
Received 29 June 2018; Received in revised form 11 October 2018; Accepted 17 October 2018
Available online 18 October 2018
0168-3659/ © 2018 Published by Elsevier B.V.

permeability properties [13]. Therefore, such a delivery vehicle offers interesting opportunities for a rational design intended to further enhance the already shown potential for oral peptide delivery.

From our perspective, another type of NCs of potential interest for oral peptide delivery is the one making use of the cationic polypeptide, protamine. These NCs, which were originally designed in our research group for nasal delivery of antigens [14], might enhance the transport of peptides across the intestinal epithelium. In fact, protamine is known to exhibit membrane-translocation properties attributed to its arginine-rich sequence [15], and because of this special property, protamine has been used, as such, for enhancing nose-to-brain delivery [16] as well as for enhancing insulin intestinal absorption [17]. In this latter work, the authors found that the systemic pharmacological bioavailability of insulin conjugated with low molecular weight protamine (LMWP) increased 5-fold compared to native insulin during *in situ* loop absorption tests in rats. Furthermore, the conjugation of insulin with the cell-penetrating LMWP followed by encapsulation in mucoadhesive nanoparticles (MNPs) resulted in a high bioavailability of insulin in diabetic rats following oral administration. The increased absorption of insulin was attributed to both the conjugation with LMWP and encapsulation in MNPs which improved the insulin penetration through the mucus and epithelial barriers [18].

Moreover, from a toxicity point of view, protamine has the advantage of being part of formulations approved by the FDA. Namely, it is used to revert the anticoagulant effects of heparin [18] and it is also part of a long-acting injectable insulin formulation [19,20].

On the other hand, taking into account the cationic charge of protamine, we found it important to explore the value of adding to the NCs an extra-layer of polysialic acid (PSA). The rationale was that, an extra layer of PSA on nanocarriers could improve the stability of the nanocapsules in the presence of proteolytic enzymes. Indeed, the presence of the hydrophilic PSA molecules on the surface of nanocarriers is expected to prevent their interaction with intestinal enzymes [21,22]. In fact, the chemical conjugation of PSA to peptides [23] or the decoration of nanocarriers using this polymer [22] are approaches that have been exploited to protect peptide molecules from degradation and improve their pharmacokinetics after parenteral administration. In addition, based on the fact that PSA is a mucus component, it was presumed that this extra-layer would facilitate the mucodiffusion of the NCs across the intestinal mucus layer.

Based on this information, the aim of this study has been to rationally design and develop protamine and protamine/PSA NCs particularly adapted for oral peptide delivery. With this aim in mind, we explored formulation strategies intended to facilitate the entrapment and the controlled release of insulin glulisine, (used as a model peptide and in this article “insulin glulisine” will simply be referred to as “insulin”), and to provide the NCs with the capacity to overcome the intestinal barriers (the lack of peptide stability in the GI tract and poor intestinal permeability). For this, we also selected auxiliary ingredients including stabilizers such as PEG-stearate and sodium glycocholate, which has an additional role as a penetration enhancer [24,25]. Finally, *in vivo* studies were performed in diabetic rats in order to elucidate the pharmacological activity of insulin loaded protamine based NCs after intra-intestinal administration.

2. Materials and methods

2.1. Materials

Protamine sulfate of low molecular weight (5 kDa), used in this work was purchased from Yuki Gosei Kogyo, Ltd., (Tokyo, Japan). The stabilizing surfactants, polyoxyethylene 40 monostearate (PEGst-40), was purchased from CRODA Europe Ltd., (Snaith, UK), whilst sodium cholate (SC) and sodium glycocholate (SGC), from Dextra, (Reading, UK). Caprylic/capric triglyceride (Miglyol® 812) was purchased from Cremer, Oleo Division, (Witten, Germany). Colominic acid sodium salt (polysialic acid, PSA) was purchased from Nacalai Tesque, INC, (Tokyo, Japan). Insulin glulisine (Apidra®, Mw 5823 Da) was kindly provided by Sanofi (Paris, France). DiD (1,1′-dioctadecyl-3,3,3′,3′-tetramethylindodicarbocyanine perchlorate) was supplied by Invitrogen (Spain). Triton x-100 was purchased from Sigma Aldrich (St. Louis, USA), whilst anhydrous monobasic sodium phosphate, maleic acid, calcium chloride, sodium oleate (purity > 82%) and acetic acid were purchased from Scharlab (Barcelona, Spain). Pancreatin (8% USP specification), was purchased from Biozym (Hamburg, Germany). Sodium taurocholate, lecithin, sodium hydroxide and glycerylmonooleate were obtained from Fluka (Buchs, Switzerland). Organic solvents were of HPLC grade and all other products used were of reagent grade purity or higher.

2.2. Cell culture

HepG2 cell line was obtained from the European Collection of Authenticated Cell Cultures (ECACC, distributed by Sigma, UK). EMEM 1 g glucose/L was purchased from Sigma, UK. Penicillin-Streptomycin and Hoechst 33258 were obtained from Sigma, Israel. FBS was purchased from GIBCO, Thermo (South America). Non-essential aminoacids were obtained from GIBCO, Thermo (Grand Island, USA), L-Glutamine from Sigma,(Brazil), Trypsin solution, from Sigma, (USA), Viafect from Promega, (Madison, USA), Turbofect from Thermo, (Lithuania), pMAXGFP from Lonza, (Köln, Germany), MW48 plates from Costar, Thermo,(New York, USA), PBS from Sigma, (St Louis MO, USA), pSynSRE-T-luc from Addgene, (Cambridge USA) and metformin from Sigma, (Steinheim Germany).

2.3. Preparation of protamine nanocapsules

Blank protamine NCs were prepared by the solvent displacement technique following the procedure described and optimized by our group [26]. Initially, for the lipid core, Miglyol®812 with a combination of different surfactants (SC, SGC, and PEGst-40) and different concentrations, were explored. Finally, for the selected formulation PEGst-40 (16 mg), SGC (5 mg) and Miglyol®812 (62.5 μL ~ 59 mg) were dissolved in 3 mL ethanol to obtain a clear lipid phase. Acetone (1.95 mL) was then added and this organic phase was immediately poured over 10 mL of an aqueous phase containing 0.15% *w/v* protamine under magnetic stirring 300 rpm. The elimination of organic solvents was performed by evaporation under vacuum (Rotavapor Heidolph, Germany), to obtain a NC formulation with a constant final volume of 5 mL. Subsequently, protamine NCs were isolated by ultracentrifugation (Optima™ L-90 K, Ultracentrifuge, Beckman Coulter, USA) at 82626 rcf for 1 h (at 15 °C) and re-suspended in ultrapure water to the initial volume. Nanoemulsions, used as controls, were prepared by the same method without incorporating protamine in the aqueous phase.

Optionally, protamine NCs were provided with an additional coating layer consisting of PSA. For this purpose, a volume of 5 mL, isolated protamine NCs (concentration 18.66 mg/mL) was incubated under magnetic stirring at 300 rpm for 30 min with a volume of 1 mL solution of PSA at a concentration 3 mg/mL. The final protamine:PSA ratio was of 5:1 (*w*/w). The concentration of NCs was determined taking into account all components in the formulation.

Insulin-loaded protamine and PSA-protamine NCs were prepared following the same procedure for blank NCs by incorporating insulin (1.0 mg, dissolved in 0.01 M HCl, 0.05 mL) into the lipid phase before mixing it with the aqueous phase containing 0.15% *w/v* protamine.

The NCs loaded with the fluorescent dye DiD, used for *in vivo* imaging studies, were prepared as described above. In this case, 0.02 mL of DiD stock solution in ethanol (2.5 mg/mL) was added to the organic phase before NCs preparation. The final concentration of DiD in the formulation was 10 μg/mL. To determine the encapsulation efficiency of DiD-loaded NCs, the system was centrifuged (82,626 rcf, 1 h, 15 °C) to eliminate the non-encapsulated dye. After this step, the

encapsulation efficiency and release were calculated indirectly by the difference between the total amount of DiD in the formulation and the free dye in the aqueous phase (undernatant). These samples were analysed at$\lambda = 646$ nm, by fluorescence spectroscopy (EnVisionMultilabel Plate Reader, Perkin Elmer, Massachusetts, MA, USA).

2.4. Physicochemical and morphological properties of protamine NCs

The average hydrodynamic diameter, and polydispersity index (PDI) of the NCs were determined by dynamic light scattering (DLS) and zeta potential was calculated from the electrophoretic mobility values determined by laser dopppler anemometry (LDA) both measured by a Zetasizer® Nano-ZS, ZEN 3600, Malvern instruments, (Worcestershire, UK) equipped with a red laser light beam ($\lambda = 632.8$ nm). For particle size and PDI measurements, the NCs were diluted 50× in milliQ water and for z-potential they were diluted 50× in 1 mM KCl. The transmission electron microscopy (TEM, Joel 2010, 80 kV, Philips, Netherlands) was used to analyse the shape and surface properties of the NCs. For TEM analysis samples were deposited on a copper grid, washed 3× with milliQ water and stained with 2% (*w/v*) phosphotungstic acid solution, allowed to dry and then viewed under TEM.

2.5. Association efficiency (AE%) and loading capacity (LC)

The association efficiency (%) was determined using the direct method, which involves the extraction of insulin from the isolated NCs by the complete disruption of the NCs. Briefly, isolated insulin-loaded NCs (0.1 mL) were digested using a combination of acetonitrile (0.1 mL), Triton™ X-100 (0.05 mL) and 0.1% TFA (0.75 mL). Then the formulation was vortexed at a high speed to obtain a clear aliquot. To corroborate this data, free insulin in the aqueous phase (undernatant) was quantified after isolating the NCs (indirect method). The concentration of insulin in both cases was determined by reverse phase liquid chromatography (HPLC).

The amount of insulin was quantified by an HPLC (Agilent model 1100 series LC equipped with a diode-array detector set at 214 nm) method in an isocratic mode. The chromatographic system was equipped with a reversed-phase 125 × 4 mm Supersphere®100 $^{-}$RP-18e-125-4 column (particle size 4 μm). The mobile phases, eluted at 1 mL/min at 44:56 *v*/v, were a mixture of phosphate buffer (0.1 M, pH 2.3) and acetonitrile (phase A 93:7 and phase B 43:57 *v*/v). The column was set at 35 °C and the injection volume was 10 μL. Calibration curves ranging from 5 μg/mL up to 1050 μg/mL ($r^2 = 0.999$) were obtained. The limit of quantification (LOQ) and limit of detection (LOD) were 200 μg/mL and 80 μg/mL, respectively. Samples were transferred into auto-sampler vials, capped and placed in the HPLC auto-sampler. Each sample was assayed in triplicate. The association efficiency (AE%) and loading capacity (LC%) were calculated using Eqs. (1) and (2) respectively:

$$\boldsymbol{AE\%} = \frac{\textbf{Insulin in destructed isolated nanocapsules}}{\textbf{Total insulin}} \times \mathbf{100} \quad (1)$$

$$\boldsymbol{LC\%} = \frac{\textbf{Total insulin} \times \textbf{AE}}{\textbf{Total weight of NCs}} \times \mathbf{100} \quad (2)$$

2.6. Conformational stability of loaded insulin

To evaluate the conformational stability of insulin against preparative stress, circular dichroism (CD) spectroscopy was used. For this study, the destruction method used in section 2.4 above, could not be applied since the presence of Triton™ X-100 interfered with the spectrum reading during analysis. For this purpose, protamine and PSA-protamine NCs were completely disrupted using a combination of chloroform, methanol and acidified milliQ water (1:1:2 *v*/v) at pH 3.46 to obtain a final concentration of insulin at 0.125 mg/mL. The aliquots were then centrifuged (Hettich, Universal 32R, Germany) at 14000 rcf for 10 min at 25 °C to obtain a clear supernatant, which was collected and analysed for insulin conformation by CD. A solution of insulin in the same medium at a concentration of 0.125 mg/mL was used as a control. Spectra were collected at 20 °C, using a 0.5 nm step size, over a wavelength range of 180–280 nm, using a 1 mm quartz cylindrical cell; a band width of 1 nm and a scanning speed of 500 nm/min, with a 0.25 s response time, were applied (Jasco J-1100; Jasco Corp, Tokyo, Japan).

The α-helical content of the protein was estimated according to the following equation:

$$\%\boldsymbol{\alpha - helical\ content} = \frac{\boldsymbol{\theta mrd - 4000}}{\mathbf{33000 - 4000}} \quad (3)$$

Where, θmrd is the mean molar ellipticity per residue at 208 nm (deg cm^2 d/mol). Raw data from the experiment, expressed in terms of θd (the ellipticity in units of mdeg) were converted to mean molar ellipticity (θmrd) per residue, using the following equation:

$$\boldsymbol{\theta mrd} = \frac{\boldsymbol{\theta d\ M}}{\mathbf{10CLN}} \quad (4)$$

Where, *M* is the insulin molecular weight (Da), *C* is the insulin concentration (mg/ mL), *L* is the sample cell path length (cm), and *N* is the number of amino residues [27].

2.7. Insulin bioactivity assay in human cells

To confirm the bioactivity of insulin after encapsulation in protamine NCs, a bioactivity assay was carried out in human cells. HepG2 cells were cultured in EMEM (1 g glucose/L, SIGMA, UK) growth medium supplemented with 10% FBS, 1% Non-essential aminoacids, 2 mM L-Glutamine, 1% Penicillin-Streptomycin. Cells were passed once per week by trypsinization for 5 min and passed through an 18-gauge needle to obtain a single cell suspension. Cells were used between passages 3 and 20.

For transfection, Viafect, and Turbofect were compared by measuring the efficiency of transfection of a commercial plasmid preparation of pMAXGFP (Lonza, Köhln Germany) following the standard recommended protocols. Efficiency was estimated by measuring the number of GFP fluorescent cells with respect to the total number of cells stained with Hoechst 33258. Apoptosis expressed as condensed Hoechst + cells was also measured and discarded for efficiency. Since Viafect obtained a > 95% efficiency while Turbofect was only 65%, all subsequent experiments were performed using Viafect.

MW48 plates were coated with 100 μg/mL Type I collagen solution in PBS then for each assay, 24,000 HepG2 cells/well were seeded in growth medium, and allowed to grow for one day. On the next day, a transfection mixture of DNA plasmid (85 ng of promoter +35 ng empty RSV plasmid/well), Viafect transfection reagent (1.5 μL/well) and EMEM (23.5 μL/well) was prepared for all wells and incubated for 20 min. Meanwhile, cell medium was replaced by growth medium plus 2 mM metformin and subsequently, 25 μL of the transfection mixture was added per well and incubated for 6 h. After washing, free insulin solution (control), protamine NCs loaded with insulin at a concentration range of 50–500 IU/mL insulin and blank protamine NCs were added to the wells. After 20 h incubation, wells were washed three times with PBS followed by addition of 40 μL Passive Lysis Buffer/well and incubation for 20 min. Lysates were collected and frozen at −20 °C. Luciferase activity was assayed as described by Garcia-Rendueles A.R., et al. [28] using 15 μL of lysate in a Mithras microplate reader (LB940, Berthold, Bad Wildbad Germany). Bioactivity data were analysed using the Kolmogorov-Smirnov normality test, followed by one way ANOVA with a posthoc multiple correction Dunnet's test, ****$p < 0.0001$.

2.8. Colloidal stability of protamine/polysialic acid NCs and release studies in simulated biological media

The colloidal stability of the NCs was assessed by monitoring the size, PDI and mean count rate (particle concentration). Different simulated intestinal media were used (prepared according to the USP XXIV) in order to mimic the intestinal environment after oral delivery. Bio-relevant media simulating pre-prandial and postprandial conditions in the upper small intestine, including fasted-state simulated intestinal fluid (FaSSIF) and fed-state simulated intestinal fluid (FeSSIF), were also employed in this study according to the updated versions-2 (V2) described by Jantratid et al. in order to mimic *in vivo* conditions. FaSSIF-V2 has a lower amount of lecithin, whereas FeSSIF-V2 combines the postprandial changes in pH, buffer capacity, osmolarity, and bile component concentrations, in addition to lipolysis products; glycerylmonooleate and sodium oleate, with *in vivo* correlating concentrations (Supplementary Table 1) [29,30].

For the stability studies, insulin loaded protamine NCs were diluted 50× and incubated under moderate horizontal (300 rpm) shaking at 37 °C in the different media: FaSSIF-V2, pH 6.5 and FeSSIF-V2, pH 5.8. Samples were collected at times 0, 0.5, 1, 3 and 6 h. The FeSSIF-V2 samples were centrifuged (Hettich, Universal 32R, Germany) at 5000 rcf for 5 min at 5 °C to eliminate pancreatin aggregates before analysis. The evolution of size distribution, PDI and mean count rate of the NCs were monitored by dynamic light scattering on a Zetasizer® Nano-ZS, Malvern, UK. The mean count rate is used as an indicator of the concentration of the tested particles and it was monitored by fixing the attenuator at 6. Three batches of the formulations were analysed and each analysis was done in triplicates.

For *in vitro* release studies, insulin loaded NCs were incubated in SIF, pH 6.8 and FaSSIF-V2, pH 6.5 at a ratio of 1:20, NCs to the medium and shaken at 100 rpm at 37 °C using a constant-temperature horizontal shaker. At specified time intervals (0, 0.25, 0.5, 1, 3, 6 and 24 h); the undernatant was collected after ultracentrifugation of the samples (section 2.2). The concentration of insulin in the undernatant was determined by reverse phase HPLC method (Section 2.4).

2.9. Insulin stability in simulated intestinal fluids containing enzymes

The ability of protamine NCs to protect the associated insulin was evaluated by quantifying the amount of insulin remaining in the NCs after proteolysis. For this purpose, insulin-loaded protamine NCs, PSA-protamine NCs and free insulin solution (as control) were diluted by 1:1 *v*/v with FeSSIF-V2 then incubated in a 37 °C incubator and shaken at 100 rpm for up to 2 h. At predetermined time intervals (0, 0.25, 0.5, 1 and 2 h), 500 μL aliquots were withdrawn and the enzyme activity of pancreatin in the samples was terminated by the addition of 300 μL ice-cold 0.1 M HCl. The samples were subsequently treated with acetonitrile (0.01 mL) and Triton x-100 (0.01 mL) and vortexed, to disrupt the NCs and extract insulin, which was then analysed by HPLC to determine the amount of insulin remaining in the NCs.

2.10. Stability during storage

The colloidal stability of insulin-loaded NCs was followed during a period of 6 months at different temperatures (4 °C, 25 °C and 40 °C) and RH conditions, as recommended by ICH guidelines. Samples of three different batches were withdrawn at predetermined time intervals, followed by determining particle size, PDI, mean count rate, zeta potential and insulin leakage coupled with observing the suspension appearance to ensure continued stability.

2.11. Freeze-drying studies

Insulin-loaded protamine NCs and PSA-protamine NCs (1% *w/v*) were lyophilized (Labconco Corp, USA) in presence/absence of trehalose or sucrose at 5% (*w/v*) as cryoprotectors. Samples were frozen at −20 °C and then subjected to an initial drying step at −40 °C followed by a secondary drying at 0 °C, both steps lasting for 43 h at a high vacuum atmosphere (200 mTorr). Finally, the temperature was increased slowly up to room temperature (+22 °C) till the end of the process. The freeze-dried formulations were re-suspended in ultrapure water by manual shaking and their physicochemical characteristics were evaluated as outlined in section 2.3.

2.12. In vivo efficacy studies in diabetic rats

Male Sprague–Dawley rats (250–300 g) were obtained from the Central Animals House, University of Santiago de Compostela (Spain). All animal experiments were reviewed and approved by the ethics committee of the University of Santiago de Compostela (procedures Prof. Carlos Dieguez, 1500AE/12/FUN01/FIS02/CDG3); performed in compliance with the Directive 2010/63/EU and Spanish Royal Decree 1201/2005, on the protection of animals used for experimental and other scientific purposes. The animals were kept under 12 h light/12 h dark cycles and were fed a standard laboratory rodent diet in pellets (Panlab A04, Panlab laboratories).

Diabetes was induced using *Streptozotocin,* where the rats were injected intraperitoneally with a single high dose of 60 mg/kg using a 1 mL syringe and 25 G gauge needle. They were monitored daily for one week before the experiment to confirm diabetes and only rats with blood glucose over 300 mg/dL were selected for the study.

The diabetic rats (average weight 267 ± 11 g) were fasted for 12 h before the experiment with free access to water. Formulations (blank protamine NCs, insulin-loaded protamine NCs) and free insulin solution were injected intrajejunally at a constant volume of 300 μL at a dose of 50 IU/kg. For this purpose, the rats were anesthetized with isoflurane gas and intra-jejunal (i.j.) administration was performance by direct injection with a 25 G gauge needle. Free insulin solution was administered subcutaneously (s.c.) at a dose of 1 IU/kg, as a positive control. Blood samples were collected from the tail vein 30 min prior to the administration, to establish the baseline blood glucose level. At time points 30 min, 1, 1.5, 2, 3, 4, 5, 6, 7, 8 h after administration, blood samples were collected to monitor the change in glucose levels. The glucose levels were measured using a hand-held glucometer (GlucocardTM G+ meter, Arkray Factory, Japan). Blood sampling was conducted without anaesthesia in freely-moving rats [6].

2.13. In vivo biodistribution studies

One week before the experiment BALB/c mice were placed on a low manganese diet to reduce auto-fluorescence. Thereafter, abdominal fur was removed by depilation and the animals were fasted 24 h before administration of the formulation. Then, 0.2 mL of isolated DiD-labeled protamine NCs (NC concentration: 18.66 mg/mL and DiD concentration of 10 μg/mL), were administered to mice by oral gavage. Free DiD at the same concentration was administered as a control. *In vivo* biodistribution was performed by total body scanning at different time points (0, 1, 3, 6, 24 h) on isoflurane/oxygen-anesthetized animals, using the Optix MX2 scanner (ART Inc., Saint-Laurent, Canada). Bioluminescent images were acquired with the OptixOptiview™ (ART Inc.) acquisition software.

To further examine the interaction of NCs with the intestinal epithelium by confocal microscopy the intestines were dissected after treatment, washed with PBS and fixed in 4% PFA for 3 to 4 h at 4 °C. Thereafter they were treated and stored at −80 °C for subsequent cryostate processing. Samples were then cut into and 10 μm thick cryoslices using a Leica CM 1850 CM cryostat and transferred to slides (SuperFrostPlus, Thermo Scientific). Confocal images were acquired with Leica TCS SP5 II microscope and further processed using ImageJ software.

2.14. Statistical analysis

Statistical analysis was performed using GraphPad Prism 6 program (CA, USA) (unless stated otherwise) applying one-way ANOVA in multiple comparisons. Differences were considered statistically significant at $*p < .05$ and all results are expressed as mean ± SD.

3. Results and discussion

In this study, protamine NCs were rationally designed to exhibit the following properties: (i) a capacity to load and control the release of insulin (ii) an adequate colloidal stability as well as the protection of the associated insulin upon exposure to simulated intestinal fluids containing enzymes; and (iii) an ability to interact with the intestinal epithelium and promote insulin absorption.

3.1. Preparation and characterization of protamine and protamine/polysialic nanocapsules

Protamine NCs are reservoir-type systems composed of an oily core surrounded by a polymeric shell made of protamine in association with surfactants. In accordance with the objective of this work, all ingredients and their organization into the NCs structure were rationally selected. The lipid core, (*i.e.* Miglyol®812 a medium chain caprylic/capric triglyceride), of the NCs was expected to help protect the peptide cargo from degradation as well as to enhance its intestinal permeability [31,32]. The surfactants selected to disperse the oil in the external water phase were PEG stearate (PEGst-40, 2 kDa) and bile salts. The presence of the PEG molecules oriented towards the external aqueous phase was thought to enhance the stability and prevent the attachment of enzymes onto the NCs [33,34], as well as promote their diffusion across the mucus [35,36]. On the other hand, two different bile salts sodium cholate (SC) and sodium glycocholate (SGC), known for their penetration enhancing properties were also selected and compared. Finally, the selection of protamine was motivated by its cell penetrating properties [14]. On the other hand, a second layer around protamine was formed with PSA, with the idea of enhancing the colloidal stability in the presence of enzymes [23].

After an extensive screening of formulation conditions (various concentrations of the ingredients, different types of bile salts and different PEG molecular weights) the formulations whose characteristics are shown in Table 2 were selected based on a number of criteria. These criteria were: reproducibility, acceptable particle size (to facilitate mucodiffusion and interaction with the underlying epithelium), neutral or negative charge (to prevent interaction with anionic enzymes and promote mucodiffusion), adequate stability during storage and upon incubation in intestinal media, as discussed later. Overall, this screening led to the definition of the composition highlighted in Fig. 1 and whose properties are presented in Table 1 and Table 2.

The results in Table 1 indicate specific compositions of NCs and their corresponding physicochemical properties, respectively. The size of the NCs was similar irrespective of the polymer forming the shell (either protamine alone or in combination with PSA), however, it was affected by the nature of the bile salt, being those made with SGC larger than the those made of SC (around 200 and 300 nm respectively). This increase in size, due to the bile salt, was not however observed in the case of the nanoemulsions. These data indicate that the way the anionic bile salt interacts with protamine is important in the formation of the NC's shell. The larger size of the SGC-containing NCs could be related to the higher negative density charge provided by SGC, as compared to SC (zeta potential values of −21 and -13 mV for SGC and SC-containing NCs). The positive charge on protamine NCs, as compared to the negatively charged control nanoemulsions, is an indicator of the presence of the protamine shell around the lipid core. Similarly, the inversion of the zeta potential values from +8 mV (Protamine NCs) to −6 mV (PSA-Protamine NCs) is an indication of the PSA coating around the protamine shell.

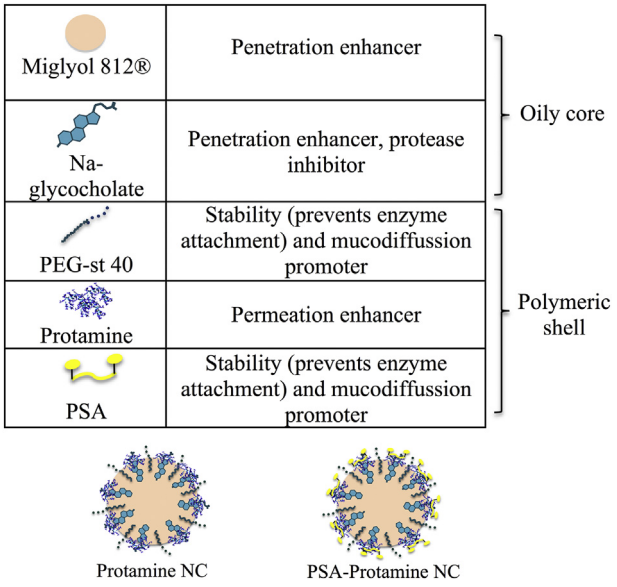

Fig. 1. Schematic representation of protamine NCs and PSA coated protamine NCs, showing the specific function/property of each component.

The size of the NCs was confirmed by TEM analysis. The images presented in Fig. 2, also illustrate the spherical shape of the NCs and different appearance of the single layer protamine NCs as compared to the double layer PSA/protamine NCs.

3.2. Insulin encapsulation and stability of the encapsulated insulin

Considering that insulin is a hydrosoluble polypeptide with and isoelectric point (IP) of 4.75, the strategy for its entrapment within the oily core was based on tuning its solubility and ionization degree using different pH media. As expected, the results shown in Table 2, indicate that both, the pH of the insulin solution and the presence of cholate bile salts influence the insulin association efficiency to the NCs ($*p < .05$). The highest AE % values were obtained when insulin was dissolved in 0.01 M NaOH, pH 9.2 in the absence of a bile salt and when insulin was dissolved in 0.01 M HCl, pH 2 in presence of SGC. These, apparently contradictory results could be explained as follows. At pH 9.2, insulin has an important net negative charge, which may help its interaction with the positively charged protamine and, thus its encapsulation is favoured in the absence of a bile salt. On the contrary, association to the NCs was highly dependent on the type of bile salt when insulin was dissolved in 0.01 M HCl. In this case, the positively charged insulin was supposed to interact with the negatively charged bile salt surfactants in the lipid core. The higher association observed for the NCs containing SGC as compared to those containing SC, might be due to the presence of the glycol moiety in the SGC molecule. In fact, the longer hydrophilic side chain has been associated with higher interaction with hydrophilic polymers(positively charged) and activity of SGC compared to SC. [37].

Regarding the effects of the amount of each of the components in the NCs on the AE % of insulin, it was observed that the presence of SGC and PEGst-40 confers advantageous properties to the system, *i.e.* acceptable size and AE % of insulin. The AE% could be modulated by adjusting the pH of the insulin solution, reaching the highest AE values when the formulation contained SGC and the pH of the insulin solution was 2. Finally, the addition of a second PSA layer led to an apparent reduction of the insulin AE, however, this difference was not statistically significant. On the other hand, the association of insulin did not have any influence on the zeta potential of the NCs. Overall, the conclusion, is that it is necessary to have an integrative analysis of the influence of the formulation parameters in order to produce NCs with

Table 1
Physicochemical properties of blank protamine and PSA-coated protamine NCs with their corresponding nanoemulsions, (mean ± SD, $n = 3$).

Control nanoemulsions				Protamine NCs			PSA-Protamine NCs		
Bile salt	Size (nm)	PI	ζ-pot (mV)	Size (nm)	PI	ζ-pot (mV)	Size (nm)	PI	ζ-pot (mV)
SC	198 ± 7	0.1	-13 ± 5	207 ± 18	0.1	+6 ± 5	200 ± 16	0.2	−4 ± 1
SGC	214 ± 15	0.2	−21 ± 2*	288 ± 20	0.2	+8 ± 4	261 ± 24	0.2	−6 ± 4

* $p < .05$ significant difference between nanoemulsions containing sodium cholate (SC) and sodium glycocholate (SGC).

the adequate characteristics.

3.3. Insulin bioactivity studies

Although the HPLC analysis used to quantify the association efficiency provided a good indication of the insulin stability (100% insulin was recovered after analysis of associated and non-associated insulin), a subsequent circular dichroism (CD) analysis was performed as the conformation of insulin is critical for its optimal therapeutic effect. Since α-helices are one of the elements of the secondary structure, the quantitative analysis of the structural change of insulin could be evaluated by the content of the preserved α-helices. The CD spectra of insulin secondary structures before and after the formulation process are shown in supplemental data Fig. 3S. The far-UV CD band at 208 nm primarily arises from the α-helix structure. The calculated percentage of α-helix in insulin (control) and insulin entrapped in protamine NCs and PSA-protamine NCs are 38.0, 36.8 and 38.4% respectively. In other words, no significant conformation change was noted after loading insulin into protamine based NCs.

Moreover, the data showing preservation of the conformational structure of the encapsulated insulin was further corroborated by *in vitro* gene expression upon the transfection of Hep2G cells. For this purpose, cells were transfected with two different plasmids, one containing response elements activated by insulin (SynSRE-T-luc) and another plasmid where these response elements are inactivated by specific mutations (SynSRE-mut-T-luc). In accordance with this, the incubation of the cells with an insulin solution gave a clear effect with the responsive plasmid whilst no effect was observed with the non-responsive plasmid (Fig. 3 A). Control experiments and the basis for the development of this study are outlined in the supplemental data and supplemental Fig. 3BS.

The study also showed that blank protamine NCs did not give any response in any of the conditions tested. On the other hand, incubation of cells with insulin-loaded protamine NCs gave a high and concentration-dependent effect with the responsive plasmid, as shown by the increasing levels of luciferase expression (Fig. 3 B). These results confirm that the insulin bioactivity was preserved during encapsulation and release from protamine NCs.

3.4. Colloidal stability of protamine-based NCs in biological fluids

To ascertain that the NCs preserve their physicochemical properties under physiological conditions we evaluated the colloidal stability of insulin-loaded NCs in simulated intestinal fluids including FaSSIF-v2 and FeSSIF-v2. The stability of the NCs was determined by monitoring the size, PDI, and count rate of the NCs using the DLS technique. Moreover, since the surface properties and composition of the NCs is known to play an important role in their stability properties, the influence of the type of bile salt and polymer coating on the stability of the NCs in the presence of enzymes was investigated. For comparison purposes a formulation without any cholic acid salt (protamine NCs without cholate) was also investigated. Results indicating that the stability of the NCs was improved by the presence of PSA and SGC are outlined in the supplemental data Fig. 4S.

3.5. In vitro release studies in simulated intestinal fluids

To corroborate the colloidal stability of the system Fig. 4 illustrates the *in vitro* release behaviour of protamine NCs and PSA-coated protamine NCs (containing PEGst-40 and SGC) in FaSSIF-V2 at pH 6.5. In this medium a biphasic release pattern with a rapid and constant insulin release, followed by a slow sustained release for up to 24 h was observed. The initial release phase could correspond to the release or diffusion of some insulin loosely associated to the shell of the NCs. This kind of biphasic profile has been previously reported for solid lipid nanoparticles (SLNs) and chitosan NCs [38,39]. Protamine NCs post-coated with PSA showed the same release profile, although the amount of insulin released in 3 h was significantly lower than that from protamine NCs.

3.6. Protection of the insulin associated to the nanocapsules from proteolysis

The ability of the NCs to preserve the associated insulin against degradation by enzymes was studied by incubating insulin-loaded protamine NCs and PSA-protamine NCs and free insulin solution (control) in FeSSIF-V2. The results in Fig. 5a indicate that, in the drastic degradation conditions chosen in this study, free insulin, was totally

Table 2
Association efficiency (AE%) and physicochemical properties of insulin loaded protamine and PSA-coated protamine NCs with insulin (IP = 4.75) at different pH, (mean ± SD, $n = 3$, *$p < .05$ statistical difference in size and in AE between HCl and NaOH).

Variations		Protamine NCs				PSA-protamine NCs			
Bile salts	pH of insulin	Size (nm)	ζ-Pot (mV)	AE%	Loading capacity%	Size (nm)	ζ-Pot (mV)	AE%	Loading capacity%
NO	9.2	425 ± 82	+2 ± 1	76 ± 9	0.8 ± 0.1	364 ± 43	−1 ± 1	48 ± 7	0.50 ± 0.1
	2.0	298 ± 83	+1 ± 2	*22 ± 5	0.24 ± 0.05	ND			
SC	9.2	287 ± 46	+3 ± 2	27 ± 5	0.29 ± 0.05	ND			
	2.0	266 ± 75	+8 ± 3	38 ± 4	0.41 ± 0.05	20 ± 14	−5 ± 3	32 ± 4	0.34 ± 0.04
SGC	9.2	295 ± 56	+4 ± 1	29 ± 2	0.31 ± 0.02	ND			
	2.0	382 ± 29	+6 ± 3	*62 ± 16	0.66 ± 0.2	321 ± 33	−4 ± 1	51 ± 6	0.54 ± 0.1

ND - not determined. For reproducibility, all measurements were carried out in at least 3 different batches (n = 3). For size and zeta potential measurements each sample was measured 3 times, each measurement with 10 runs and each run lasted for 10 s. The cut-off diameter was 500 nm. These parameters were pre-set in the Zetasizer and remained consistent for all measurements.

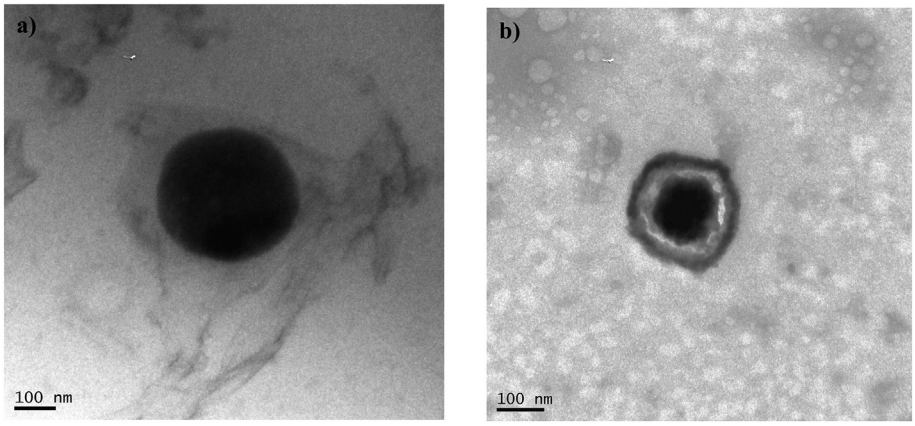

Fig. 2. TEM images of blank protamine NCs (a) and PSA-coated protamine NCs (b).

degraded in the first 15 min. In contrast, insulin entrapped into protamine NCs was highly preserved from degradation, maintaining between 55 and 75% insulin in the same period of time (15 min). Moreover, the presence of bile salts, and notably SGC in the NCs, significantly contributed to enhancing the stability of the encapsulated insulin. This stabilizing role of the NCs was even more pronounced when they were provided with the external coating of PSA (Fig. 5b). This behaviour, expected in the rational design of the NCs, was attributed to the shielding effect of the PSA layer, which could be able to reduce the attachment of the degrading enzymes [22]. Moreover, both PSA and SGC could have a role in terms of inhibiting protease activity [40].

Overall, protamine NCs containing bile salts in their polymer shell showed a potential for the effective protection of insulin and this property was enhanced by the presence of an additional coating layer of PSA. It should also be taken into account that some of the observed insulin degradation could be attributed to its release in the medium as opposed to complete disintegration of the nanosystem as observed in section 3.5.

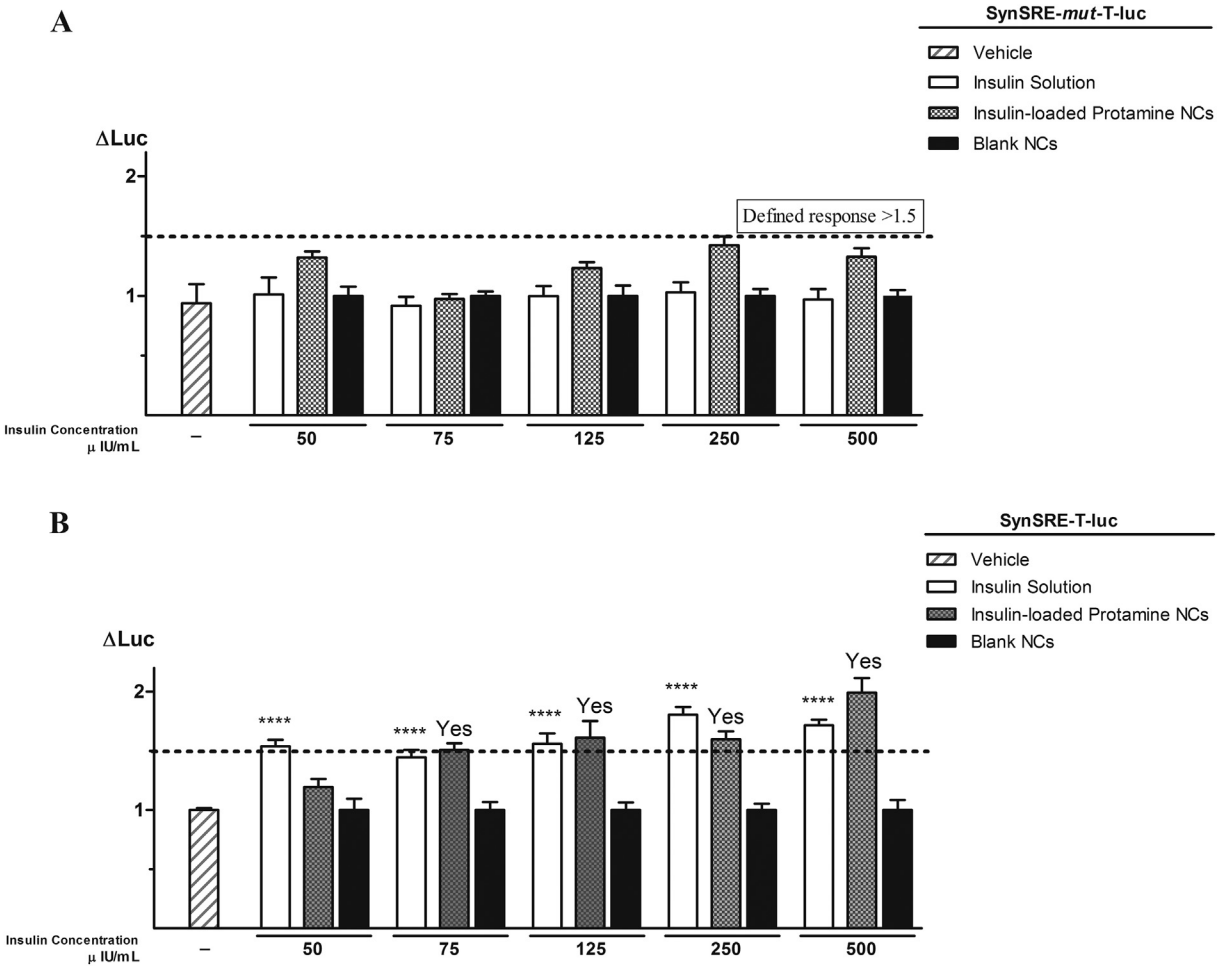

Fig. 3. Bioactivity of free insulin solution, blank protamine NCs and Insulin-loaded protamine NCs in HepG cells. Mean ± SEM, $n = 8$. "Vehicle" denotes the insulin dissolution medium alone (*i.e.* without any insulin nor NCs).

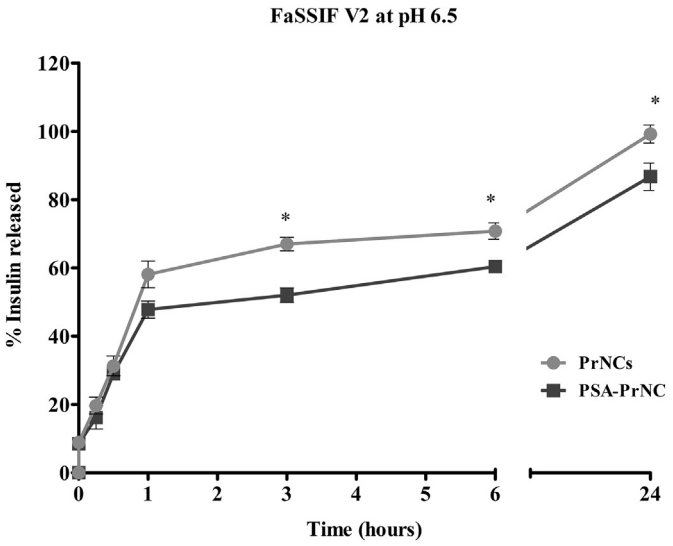

Fig. 4. *In vitro* release profiles of insulin from protamine NCs and PSA-protamine NCs incubated in FaSSIF-V2 (B), (mean ± SD, $n = 3$, $*p < .05$).

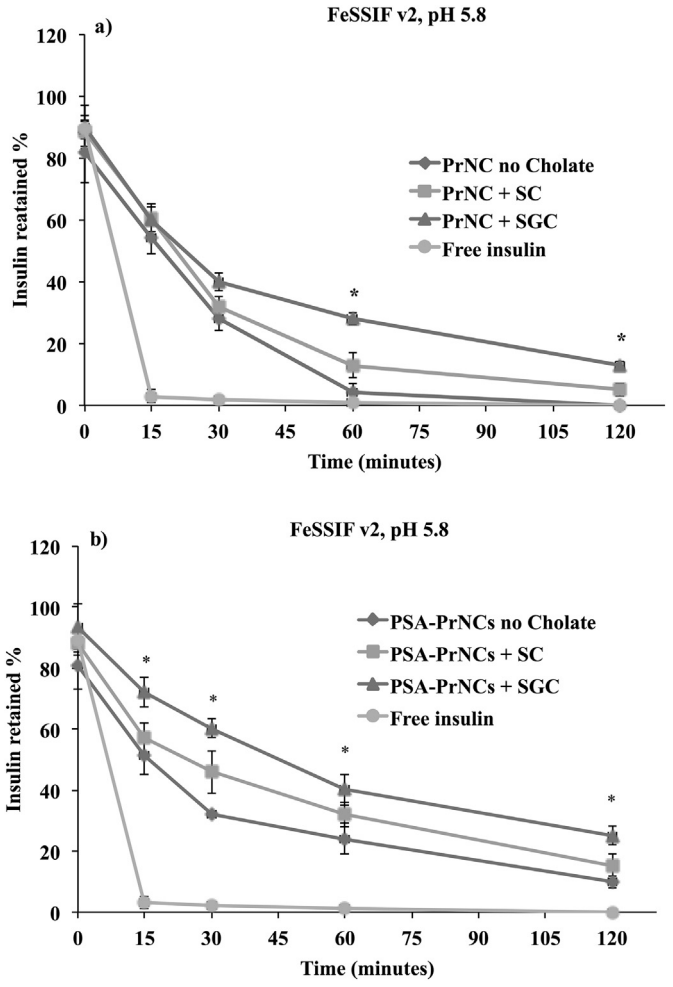

Fig. 5. Stability profiles of the associated insulin after incubation of (a) Protamine NCs and (b) PSA coated Protamine NCs in FeSSIF-V2 (mean ± SD, $n = 3$, $*p < .05$ significant difference of PrNCs + SGC compared to PrNCs without cholate).

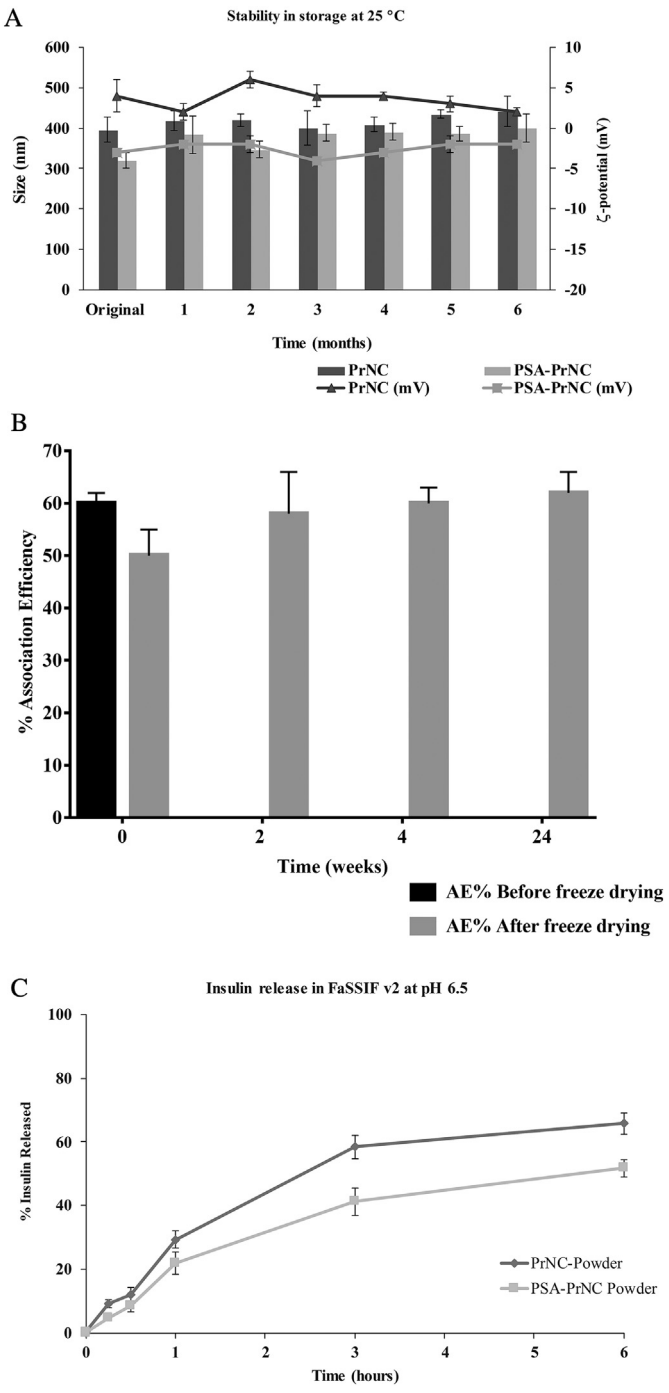

Fig. 6. (a, b and c) Physicochemical properties and insulin release profile of freeze-dried protamine NCs and PSA-protamine NCs stored at 25 °C ± 2 °C/ 60% ± 5% RH (mean ± SD, $n = 3$).

3.7. Freeze drying of the nanocapsules suspension and stability of the freeze-dried powder during storage

The conversion of the colloidal NCs into a dried state was considered as a strategy to further incorporate the NCs into a solid dosage form [41]. In this study, different concentrations of insulin-loaded PSA coated and non-coated protamine NCs with SGC were freeze-dried in presence and/or absence of cryoprotectants (trehalose or sucrose at 5%). As shown in supplementary data (Fig. 1a and b), the reconstituted powders of both formulations protamine NCs and PSA-protamine NCs, maintained their initial nanometric properties even without the use of

cryoprotectants. Therefore, the presence of the protamine coat and the combined PSA-protamine coat around the oily core of the NCs play an important protective role during freeze-drying [42].

Finally, the effect of storage temperature and relative humidity on the stability of freeze-dried NCs was tested, according to ICH conditions and guidelines. Freeze-dried insulin loaded protamine NCs and PSA-protamine NCs were kept at 25 °C ± 2 °C / 60% ± 5% RH, and their physicochemical properties were monitored and recorded over a period of 6 months. Fig. 6(a) and (b) show that the physicochemical properties including the EE% of the NCs of insulin-loaded protamine NCs did not change during the period of the study. Moreover, converting protamine based NCs into powder also improved their *in vitro* release profile (Fig. 6 (c)) by improving the controlled release and reducing the amount of insulin initially released in the first 30 min (compared to NCs in suspension, Fig. 4). This change in the release behaviour could be associated to the compaction of the NC's shell during the freeze-drying process. This is a very promising feature for this nanocarrier system as it shows that converting the NCs into powder enhances their controlled release capacity and stability.

3.8. In vivo performance of the nanocapsules

The *in vitro* studies clearly underlined the value of our rational design of protamine-based NCs. Indeed, the developed NC formulations fulfilled several criteria, such as stability in simulated GI fluids with a controlled release profile for insulin. Based on these promising properties, we studied the *in vivo* efficacy of the protamine NCs in diabetic rats in order to assess the glucose response after insulin administration in hyperglycaemic status.

Surprisingly, in initial preliminary experiments we observed that despite the positive results on the *in vitro* characterization of PSA-Protamine Nanocapsules, the external PSA coating did not contribute to the performance of the nanocapsules (results not shown). Therefore, the results reported in Fig. 7–8, refer to Protamine nanocapsules.

As shown in Fig. 7, after the subcutaneous administration of insulin solution (1 IU/Kg), as positive control, glucose levels significantly decreased by 40 to 70% after 1 to 2 h. On the other hand, the administration of aqueous insulin solution intra-intestinally, at a dose of 50 IU/kg, did not yield any significant variation on the blood glucose levels. This observation is attributed to the rapid degradation of insulin in the intestinal fluid and its poor permeability through epithelia [7]. The administration of insulin-loaded protamine NCs on the other hand, generated a remarkable hypoglycemic response with maximal 50 to 60% of reduction in blood glucose levels after 3 h. The slow onset and long-acting effect of insulin loaded protamine NCs suggest a controlled release of insulin from the core-shell corona structure of the NCs, a phenomenon already observed during *in vitro* release studies in simulated intestinal fluid (FaSSIF-v2), where 50% of the encapsulated insulin was only released after an hour, followed by a controlled (constant) release over a period of 6 h and lasted up to even 24 h [27]. These results demonstrated that insulin encapsulated in protamine NCs exhibited prolonged hypoglycemic activity without the initial drastic hypoglycaemia seen with *sc.* administration, suggesting that protamine NCs maybe a promising strategy for clinical treatment of diabetes.

*$p < .05$ for insulin loaded protamine NCs compared to the free insulin s.c. control, $\$p < .05$ for insulin loaded protamine NCs compared to the free insulin i.j.

In order to elucidate the *in vivo* fate of the NCs, which could also shed light on the observed *in vivo* behaviour, we studied the system's *in vivo* biodistribution and interaction with the intestinal epithelium in mice using IVIS and confocal microscopy of intestine sections. The images obtained for representative mice are shown in Fig. 8. These bioluminescent images suggest that both the protamine NCs and free-DiD dye are confined in the gastro-intestinal tract (mainly in the stomach and small intestines) for up to 24 h. However, the florescence intensity shows evidence of greater retention of protamine NCs as compared to the free dye (control) during the period of the study.

Further analysis of the interaction of the fluorescent NCs with the intestinal mucosa was performed by dissecting the intestines of mice at 1 h after oral administration of the NCs. As shown in Fig. 8, at this time-point, protamine NCs were observed within the mucus layer covering the intestinal villi, implying that protamine NCs had not diffused sufficiently through the mucus at this early time point. It is generally accepted that protamine is a cell penetrating polypeptide taken up by the intestinal epithelium and can lead to a gradient diffusion of insulin from the high concentration of NCs matrix towards the intestinal cells [43]. Thus, the uptake of NCs with this polymer matrix is potentially facilitated [44]. Nevertheless, this observation was made only one hour after administration and, hence further studies are needed to have a better understanding of the fate of these NCs [45].

Overall, these *in vivo* data suggest that protamine NCs are able to provide a considerable and long-lasting effect on the blood glucose levels following intra-intestinal administration. Nevertheless, the biodistribution data suggesting limited permeation of the NCs across the

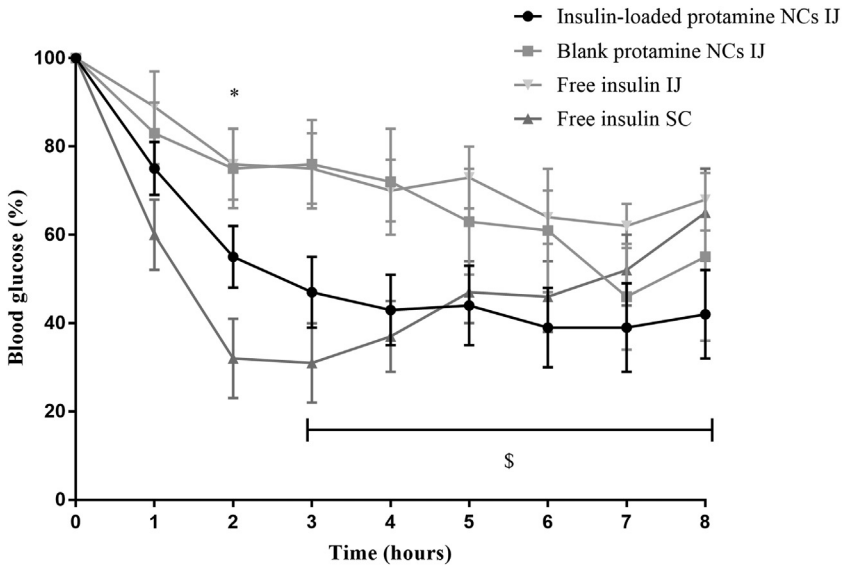

Fig. 7. Standardized hypoglycemic effect following intra-jejunal administration of insulin-loaded protamine NCs (50 IU/kg, $n = 14$), blank protamine NCs (placebo, $n = 8$) and insulin saline solution as intrajejunal injection (50 IU/kg, $n = 17$) and as subcutaneous injection 1 IU/kg n = 14) in diabetic rats. Mean ± SEM.

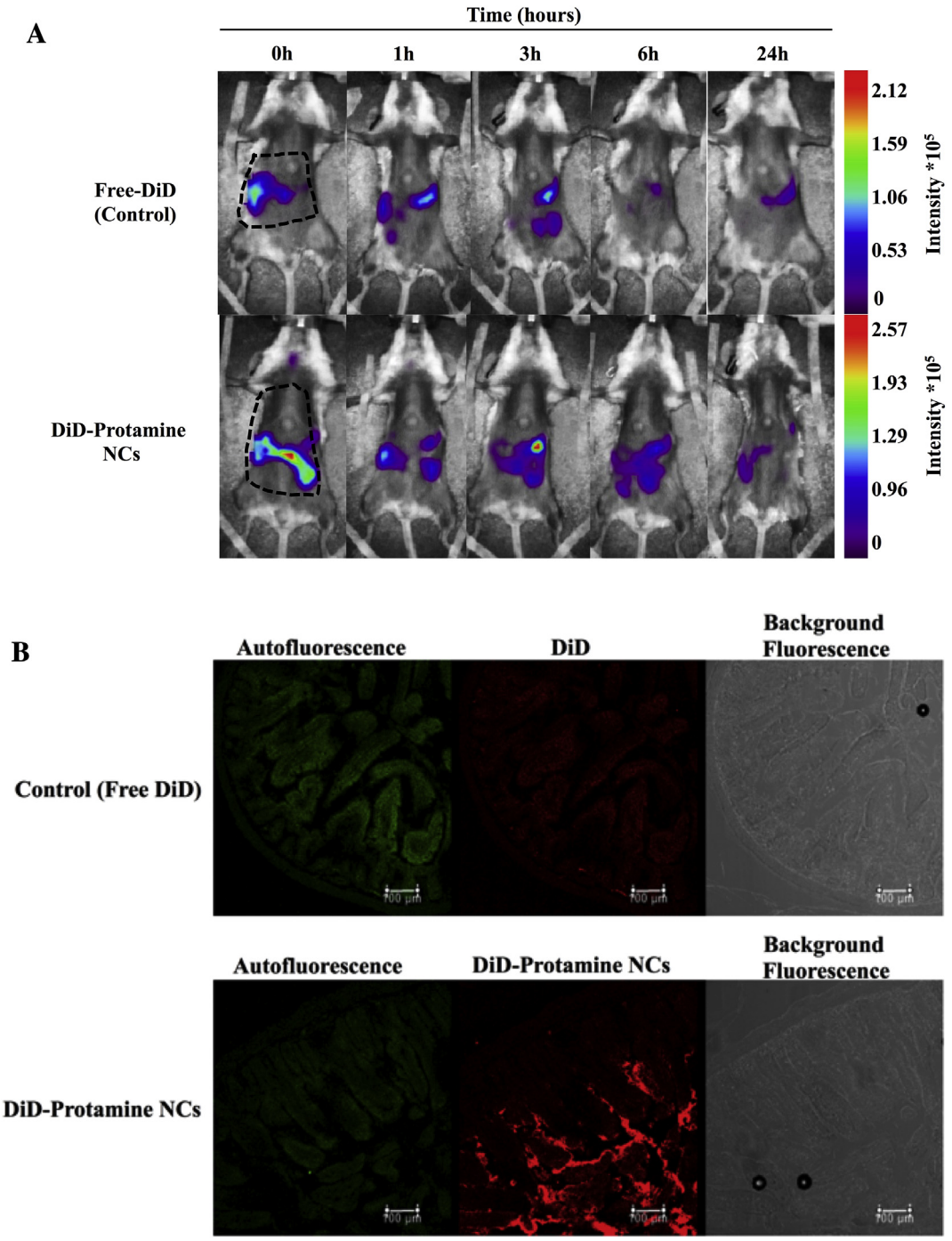

Fig. 8. a. Representative fluorescence images of mice at 0 h, 1 h, 3 h, 6 h and 24 h following oral administration of free-DiD control (top) and DiD-labeled protamine NCs (down). b. Confocal images showing the interaction of (i) free DiD (control) and (ii) DiD-protamine NCs with mouse intestinal tissue (duodenum) 1 h after oral administration. (20 x magnification with air objectives).

mucosa, still raises the possibility to further improve the *in vivo* performance of protamine NCs, probably by reducing their size, thereby improving their mucodiffusion across the intestinal mucosa.

4. Conclusions

In this work we report NCs consisting of an oily core and a single or double layer consisting of protamine/PSA as a delivery system for the oral administration of peptides. These NCs, which were rationally designed in order to confer them with the capacity to withstand the multiple barriers associated to the intestinal tract, were also able to load a significant amount of insulin and control its release in simulated intestinal media containing bile salts and proteolytic enzymes. Moreover, the NCs could be converted into a powder that was stable at room temperature for at least 6 months. The results obtained following insulin bioactivity assay in human cells of insulin-loaded protamine NCs confirmed that the bioactivity of the insulin is preserved, whilst intra-intestinal administration of the formulation, led to a significant reduction of the glucose levels. The data presented here provide a preliminary efficacy proof of concept of oral insulin delivery using protamine NCs.

Acknowledgements

The authors appreciate Maria Suarez-Farina for her technical expertise in the insulin bioactivity assays. The research leading to this publication has received funding from the European Union Seventh Framework Programme (FP7/2007-2013) under grant agreement n° 281035 (TRANSINT). The first author, L.N. Thwala acknowledges her doctoral fellowship from the European Commission, Education, Audiovisual and Culture Executive Agency (EACEA), under the Erasmus Mundus programme, "NanoFar: European Doctorate in Nanomedicine and Pharmaceutical Innovation" (ref: 2012 0028). The authors declare no potential conflict of interest regarding the content of this work. They have no other relevant affiliations or financial involvement with any organization or entity with a financial interest in or financial conflict with the subject matter or materials discussed in the manuscript apart from those disclosed.

Appendix A. Supplementary data

Supplementary data to this article can be found online at https://doi.org/10.1016/j.jconrel.2018.10.022.

References

[1] B.F. Choonara, Y.E. Choonara, P. Kumar, D. Bijukumar, L.C. du Toit, V. Pillay, A review of advanced oral drug delivery technologies facilitating the protection and absorption of protein and peptide molecules, Biotechnol. Adv. 32 (2014) 1269–1282, https://doi.org/10.1016/j.biotechadv.2014.07.006.

[2] A.W. Du, M.H. Stenzel, Drug carriers for the delivery of therapeutic peptides, Biomacromolecules 15 (2014) 1097–1114, https://doi.org/10.1021/bm500169p.

[3] L.N. Thwala, V. Préat, N.S. Csaba, Emerging delivery platforms for mucosal administration of biopharmaceuticals: a critical update on nasal, pulmonary and oral routes, Expert Opin. Drug Deliv. 14 (2017), https://doi.org/10.1080/17425247.2016.1206074.

[4] M. Niu, Y. Lu, L. Hovgaard, P. Guan, Y. Tan, R. Lian, J. Qi, W. Wu, Hypoglycemic activity and oral bioavailability of insulin-loaded liposomes containing bile salts in rats: the effect of cholate type, particle size and administered dose, Eur. J. Pharm. Biopharm. 81 (2012) 265–272, https://doi.org/10.1016/j.ejpb.2012.02.009.

[5] J. Mudassir, Y. Darwis, P.K. Khiang, Prerequisite characteristics of nanocarriers favoring oral insulin delivery: nanogels as an opportunity, Int. J. Polym. Mater. Polym. Biomater. 64 (2015) 155–167, https://doi.org/10.1080/00914037.2014.921919.

[6] P. Fonte, T. Nogueira, C. Gehm, D. Ferreira, B. Sarmento, Chitosan-coated solid lipid nanoparticles enhance the oral absorption of insulin, Drug Deliv. Transl. Res. 1 (2011) 299–308, https://doi.org/10.1007/s13346-011-0023-5.

[7] P. Fonte, F. Araújo, C. Silva, C. Pereira, S. Reis, H.a. Santos, B. Sarmento, Polymer-based nanoparticles for oral insulin delivery: revisited approaches, Biotechnol. Adv. (2015), https://doi.org/10.1016/j.biotechadv.2015.02.010.

[8] K. Yoncheva, L. Guembe, M.A. Campanero, J.M. Irache, Evaluation of bioadhesive potential and intestinal transport of pegylated poly(anhydride) nanoparticles, Int. J. Pharm. 334 (2007) 156–165, https://doi.org/10.1016/j.ijpharm.2006.10.016.

[9] A. Makhlof, M. Werle, Y. Tozuka, H. Takeuchi, A mucoadhesive nanoparticulate system for the simultaneous delivery of macromolecules and permeation enhancers to the intestinal mucosa, J. Control. Release 149 (2011) 81–88, https://doi.org/10.1016/j.jconrel.2010.02.001.

[10] C. Damge, C. Michel, M. Aprahamian, P. Couvreur, New approach for oral administration of insulin with polyalkylcyanoacrylate nanocapsules as drug carrier, Diabetes 37 (1988) 246–251, https://doi.org/10.2337/diabetes.37.2.246.

[11] C. Prego, D. Torres, M.J. Alonso, The potential of chitosan for the oral administration of peptides, Expert Opin. Drug Deliv. 2 (2005) 843–854, https://doi.org/10.1517/17425247.2.5.843.

[12] C. Damgé, C. Michel, M. Aprahamian, P. Couvreur, J.P. Devissaguet, Nanocapsules as carriers for oral peptide delivery, J. Control. Release 13 (1990) 233–239, https://doi.org/10.1016/0168-3659(90)90013-J.

[13] W. Shan, X. Zhu, M. Liu, L. Li, J. Zhong, W. Sun, Z. Zhang, Y. Huang, Overcoming the Diffusion Barrier of Mucus and Absorption Barrier of Epithelium by Self-Assembled Nanoparticles for Oral Delivery of Insulin, ACS Nano 9 (2015) 2345–2356, https://doi.org/10.1021/acsnano.5b00028.

[14] J.V. González-Aramundiz, M.P. Olmedo, Á. González-Fernández, M.J.A. Fernández, N.S. Csaba, Protamine-based nanoparticles as new antigen delivery systems, Eur. J. Pharm. Biopharm. 97 (2015) 51–59, https://doi.org/10.1016/j.ejpb.2015.09.019.

[15] F. Reynolds, R. Weissleder, L. Josephson, Protamine as an efficient membrane-translocating peptide, Bioconjug. Chem. 16 (2005) 1240–1245, https://doi.org/10.1021/bc0501451.

[16] H. Xia, X. Gao, G. Gu, Z. Liu, N. Zeng, Q. Hu, Q. Song, L. Yao, Z. Pang, X. Jiang, J. Chen, H. Chen, Low molecular weight protamine-functionalized nanoparticles for drug delivery to the brain after intranasal administration, Biomaterials 32 (2011) 9888–9898, https://doi.org/10.1016/j.biomaterials.2011.09.004.

[17] H. He, J. Sheng, A.E. David, Y.M. Kwon, J. Zhang, Y. Huang, J. Wang, V.C. Yang, The use of low molecular weight protamine chemical chimera to enhance monomeric insulin intestinal absorption, Biomaterials 34 (2013) 7733–7743, https://doi.org/10.1016/j.biomaterials.2013.06.047.

[18] J. Sheng, H. He, L. Han, J. Qin, S. Chen, G. Ru, R. Li, P. Yang, J. Wang, V.C. Yang, Enhancing insulin oral absorption by using mucoadhesive nanoparticles loaded with LMWP-linked insulin conjugates, J. Control. Release 233 (2016) 181–190, https://doi.org/10.1016/j.jconrel.2016.05.015.

[19] E. Pharmacopoeia, I. Units, L. The, C. Add, D. Heat, T.S.S. Dissolve, D. Prepare, D. Protamine, Protamine sulphate protamini sulfas protirelinum, TEST 85 (n.d.) 2334–2335.

[20] J.F. Liang, L. Zhen, L.-C. Chang, V.C. Yang, A less toxic heparin antagonist–low molecular weight protamine, Biochemistry (Mosc) 68 (2003) 116–120.

[21] T. Yin, L. Yang, Y. Liu, X. Zhou, J. Sun, J. Liu, Sialic acid (SA)-modified selenium nanoparticles coated with a high blood-brain barrier permeability peptide-B6 peptide for potential use in Alzheimer's disease, Acta Biomater. 25 (2015) 172–183, https://doi.org/10.1016/j.actbio.2015.06.035.

[22] T. Zhang, Z. She, Z. Huang, J. Li, X. Luo, Y. Deng, Application of sialic acid/polysialic acid in the drug delivery systems, Asian J. Pharm. Sci. 9 (2014) 75–81, https://doi.org/10.1016/j.ajps.2014.03.001.

[23] G. Gregoriadis, S. Jain, I. Papaioannou, P. Laing, Improving the therapeutic efficacy of peptides and proteins: A role for polysialic acids, 300 (2005) 125–130, https://doi.org/10.1016/j.ijpharm.2005.06.007.

[24] M. García-Fuentes, D. Torres, M.J. Alonso, Design of lipid nanoparticles for the oral deli v ery of hydrophilic macromolecules, Colloids Surfaces B Biointerfaces. 27 (2002) 159–168.

[25] E. Moghimipour, A. Jalali, S. Abolghassem, S. Tabassi, The Enhancing Effect of Sodium Glycocholate and Sodium Salicylate on Rats Gastro-intestinal Permeability to Insulin, (2004), pp. 87–91.

[26] P. Calvo, C. Remunan-Lopez, Development of positively charged colloidal drug carriers:chitosan-coated polyester nanocapsules and submicron-emulsions, Colloid Polym. Sci. 275 (1997) 46–53, https://doi.org/10.1007/s003960050050.

[27] S. Shu, X. Zhang, D. Teng, Z. Wang, C. Li, Polyelectrolyte nanoparticles based on water-soluble chitosan-poly(L-aspartic acid)-polyethylene glycol for controlled protein release, Carbohydr. Res. 344 (2009) 1197–1204, https://doi.org/10.1016/j.carres.2009.04.018.

[28] A.C. Garcia-Rendueles Ar, Rodrigues JS, Garcia-Rendueles ME, Suarez-Fariña M, Perez-Romero S, Barreiro F, Bernabeu I, Rodriguez-Garcia J, Fugazzola L, Sakai T, Liu F, Cameselle-Teijeiro J, Bravo SB, Rewiring of the apoptotic TGF-β-SMAD/NFκB pathway through an oncogenic function of p27 in human papillary thyroid cancer., Oncogene 5 (2017) 652–666. doi:https://doi.org/10.1038/onc.2016.233. Epub 2016 Jul 25.

[29] E. Jantratid, N. Janssen, C. Reppas, J.B. Dressman, Dissolution media simulating conditions in the proximal human gastrointestinal tract: an update, Pharm. Res. 25 (2008) 1663–1676, https://doi.org/10.1007/s11095-008-9569-4.

[30] E. Jantratid, J. Dressman, Simulating the proximal human gastrointestinal tract: an update, Dissolution Technol. (2009) 21–25 http://www.dissolutiontech.com/DTresour/200908Articles/DT200908_A03.pdf.

[31] B. Marten, M. Pfeuffer, J. Schrezenmeir, Medium-chain triglycerides, Int. Dairy J. 16 (2006) 1374–1382, https://doi.org/10.1016/j.idairyj.2006.06.015.

[32] K.A. Traul, A. Driedger, D.L. Ingle, D. Nakhasi, Review of the toxicologic properties of medium-chain triglycerides, Food Chem. Toxicol. 38 (2000) 79–98, https://doi.org/10.1016/S0278-6915(99)00106-4.

[33] M.J. Taylor, S. Tanna, T. Sahota, In vivo study of a polymeric glucose-sensitive insulin delivery system using a rat model, J. Pharm. Sci. 99 (2010) 4215–4227, https://doi.org/10.1002/jps.

[34] S. Parveen, S.K. Sahoo, Long circulating chitosan/PEG blended PLGA nanoparticle for tumor drug delivery, Eur. J. Pharmacol. 670 (2011) 372–383, https://doi.org/10.1016/j.ejphar.2011.09.023.

[35] L.M. Ensign, R. Cone, J. Hanes, Oral drug delivery with polymeric nanoparticles: the gastrointestinal mucus barriers, Adv. Drug Deliv. Rev. 64 (2012) 557–570, https://doi.org/10.1016/j.addr.2011.12.009.

[36] A. Vila, H. Gill, O. McCallion, M.J. Alonso, Transport of PLA-PEG particles across the nasal mucosa: effect of particle size and PEG coating density, J. Control. Release 98 (2004) 231–244, https://doi.org/10.1016/j.jconrel.2004.04.026.

[37] R. Holm, A. MuÏLertz, H. Mu, Bile salts and their importance for drug absorption, Int. J. Pharm. 453 (2013) 44–55, https://doi.org/10.1016/j.ijpharm.2013.04.003.

[38] J. Liu, T. Gong, C. Wang, Z. Zhong, Z. Zhang, Solid lipid nanoparticles loaded with insulin by sodium cholate-phosphatidylcholine-based mixed micelles: Preparation and characterization, Int. J. Pharm. 340 (2007) 153–162, https://doi.org/10.1016/j.ijpharm.2007.03.009.

[39] C. Prego, D. Torres, E. Fernandez-Megia, R. Novoa-Carballal, E. Quiñoá, M.J. Alonso, Chitosan–PEG nanocapsules as new carriers for oral peptide delivery, J. Control. Release 111 (2006) 299–308, https://doi.org/10.1016/j.jconrel.2005.12.015.

[40] T. Taniguchi A Yamamoto, K. Rikyuu, T. Tsuji, T. Fujita, M. Murakami, S. Muranishi, Effects of various protease inhibitors on the intestinal absorption and degradation of insulin in rats, Pharm. Res. 11 (1994) 1496–1500, https://doi.org/10.1023/A:1018968611962.

[41] W. Abdelwahed, G. Degobert, H. Fessi, Investigation of nanocapsules stabilization by amorphous excipients during freeze-drying and storage, Eur. J. Pharm. Biopharm. 63 (2006) 87–94, https://doi.org/10.1016/j.ejpb.2006.01.015.

[42] C. Prego, M. García, D. Torres, M.J. Alonso, Transmucosal macromolecular drug delivery, J. Control. Release 101 (2005) 151–162, https://doi.org/10.1016/j.jconrel.2004.07.030.

[43] L.N. Thwala, A. Beloqui, N.S. Csaba, D. González-Touceda, S. Tovar, C. Dieguez,

M.J. Alonso, V. Préat, The interaction of protamine nanocapsules with the intestinal epithelium: A mechanistic approach, J. Control. Release 243 (2016), https://doi.org/10.1016/j.jconrel.2016.10.002.
[44] C. Damgé, J. Vonderscher, P. Marbach, M. Pinget, Poly(alkyl cyanoacrylate) nanocapsules as a delivery system in the rat for octreotide, a long-acting somatostatin analogue, J. Pharm. Pharmacol. 49 (1997) 949–954 http://www.ncbi.nlm.nih.gov/pubmed/9364401.
[45] L. Inchaurraga, N. Martín-Arbella, V. Zabaleta, G. Quincoces, I. Peñuelas, J.M. Irache, In vivo study of the mucus-permeating properties of PEG-coated nanoparticles following oral administration, Eur. J. Pharm. Biopharm. 97 (2015) 280–289, https://doi.org/10.1016/j.ejpb.2014.12.021.